

# Mixed-Ligand Oxidovanadium(V) Complexes with *N'*-Salicylidenehydrazides: Synthesis, Structure, and $^{51}\text{V}$ Solid-State MAS NMR Investigation

Simona Nica,<sup>[a]</sup> Axel Buchholz,<sup>[a]</sup> Manfred Rudolph,<sup>[a]</sup> Annika Schweitzer,<sup>[b]</sup> Maria Wächtler,<sup>[b]</sup> Hergen Breitzke,<sup>[b]</sup> Gerd Buntkowsky,<sup>[b]</sup> and Winfried Plass\*<sup>[a]</sup>

*Dedicated to Professor Achim Müller on the occasion of his 70th birthday*

**Keywords:** 8-Hydroxyquinoline / Schiff bases / Square-wave voltammetry / Vanadium /  $^{51}\text{V}$  NMR spectroscopy

The synthesis and spectroscopic characterization of a series of three oxidovanadium(V) complexes with 8-hydroxyquinoline and Schiff-base ligands derived from salicylaldehyde and  $\omega$ -hydroxy-functionalized carbohydrazides with different chain lengths are reported. The complex with the hydrazone ligand containing the shortest chain length was crystallographically characterized. This complex crystallizes in the triclinic space group  $P\bar{1}$  with two structurally similar but crystallographically independent oxidovanadium(V) complexes. Each vanadium atom is six-coordinate in a distorted-octahedral geometry. The two molecules are assembled through hydrogen-bonding interactions between the hydroxyl groups of the side-chain substituted Schiff-base ligand and the oxido group of one of the two complexes. Electrochemical measurements performed in acetonitrile solution reveal two reversible one-electron reduction steps.

The observed pre-wave feature of the second reduction step indicates the presence of dissociation equilibria related to the 8-hydroxyquinoline coligand. Magic-angle spinning solid-state  $^{51}\text{V}$  NMR spectroscopy allowed to characterize the full series of complexes with alkyl and hydroxy alkyl-substituted hydrazone ligands that were used. The quadrupolar coupling constants are small with a value of about 4 MHz and show little variation within the series. The asymmetry of the chemical shift tensor indicates a rather axial symmetric environment around the vanadium(V) center. The isotropic chemical shifts observed in the solid state occur at about 30 ppm, which is in the same order of magnitude as the solvent induced variations, about 10 ppm, found for different solvents.

(© Wiley-VCH Verlag GmbH & Co. KGaA, 69451 Weinheim, Germany, 2008)

## Introduction

There is a continuous interest in the coordination chemistry of vanadium due to its catalytic and medicinal importance.<sup>[1]</sup> Besides the insulin-like activity of oxidovanadium(V) and oxidovanadium(IV) compounds,<sup>[2,3]</sup> its presence in vanadium-dependent haloperoxidases<sup>[4–6]</sup> in particular has stimulated the search for structural and functional models. In this context pentavalent-vanadium complexes with the  $\{\text{VO}^{3+}\}$ <sup>[7–12]</sup> and  $\{\text{VO}_2^+\}$ <sup>[13–16]</sup> core motifs have received considerable attention. Moreover, the ability of ascidians to accumulate vanadium has initiated a rich chemistry related to its reduced states.<sup>[1,17]</sup> This particularly includes 8-hydroxyquinoline complexes, which exhibit an interesting electrochemistry.<sup>[18–20]</sup> The corresponding bis(8-hydroxyquinolinato)vanadium(V) complexes have been ex-

plored leading to a series of derivatives viewed as inorganic analogs of carboxylic acids.<sup>[21]</sup>

We could recently show that *N'*-salicylidenehydrazides are versatile ligand systems supporting different types of vanadium(V) complexes,<sup>[15]</sup> which is a result of this ligand system being prone to variable protonation states at the amide group.<sup>[22–24]</sup> Moreover, these systems can easily be modified by the introduction of various functional groups attached to the ligand core.<sup>[25–27]</sup> A particular feature is the formation of intramolecular hydrogen-bonding interactions with the vanadate moiety, in this case a hydroxy functionalized side chain.<sup>[28,29]</sup>

In the present work, we report on a series of mixed-ligand oxidovanadium(V) complexes containing the  $\omega$ -hydroxy functionalized *N'*-salicylidenehydrazide ligand system together with the electrochemically interesting 8-hydroxyquinoline as a coligand. In addition to their electrochemical properties we also investigated these compounds by  $^{51}\text{V}$  solid-state NMR spectroscopy. The latter has proven to be an excellent probe to gain quantitative site-specific information for amorphous and crystalline solids, in bulk, on surfaces, and at the interfaces.<sup>[30–34]</sup>

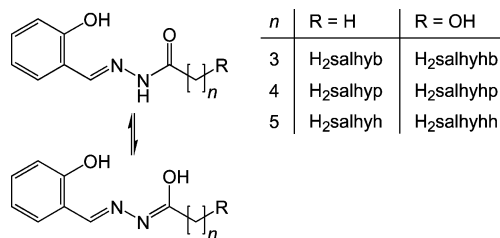
[a] Institut für Anorganische und Analytische Chemie, Friedrich-Schiller-Universität Jena, Carl-Zeiss-Promenade 10, 07745 Jena, Germany  
Fax: +49-3641-948132  
E-mail: Sekr.Plass@uni-jena.de

[b] Institut für Physikalische Chemie, Friedrich-Schiller-Universität Jena, Helmholtzweg 4, 07743 Jena, Germany

## Results and Discussion

### Synthesis and Characterization

The Schiff-base ligands with a  $\omega$ -hydroxy-functionalized side chain, used in the present work, have been prepared by condensation of salicylaldehyde with the appropriate carbohydrazides ( $H_2$ salhyhb,  $H_2$ salhyhp, and  $H_2$ salhyhh; see Scheme 1). This affords tridentate-chelate ligands with a variable protonation state at the amide function, which can therefore act as mono- and dianionic systems.<sup>[22–24]</sup> The reaction of equimolar amounts of the Schiff-base ligand with vanadyl acetylacetonate in methanol under reflux and aerobic conditions leads to a color change of the initially green reaction mixture to a brown solution, indicating the formation of a vanadium(V) species. Subsequent addition of the coligand 8-hydroxyquinoline affords dark-violet reaction solutions from which the mixed-ligand oxidovanadium(V) complexes [VO(salhyhb)(hq)], [VO(salhyhp)(hq)], and [VO(salhyhh)(hq)] can be isolated. Alternatively, this reaction sequence can also be performed in acetonitrile leading to somewhat higher overall reaction yields. The obtained complexes show very good solubility in a broad range of organic solvents like alcohols, DMF, DMSO, chloroform, dichloromethane, and acetonitrile. It should be noted here that attempts to utilize ammonium metavanadate in methanol solution directly as a vanadium(V) precursor did not lead to the desired complexes, but instead afforded a mixture of the corresponding ammonium salt of the *cis*-dioxidovanadium(V) complexes<sup>[15,28]</sup> and bis(8-hydroxyquinolino)methoxyxidovanadium(V).



Scheme 1.

The formation of an oxidovanadium(V) moiety in the synthesized mixed-ligand complexes is confirmed by their IR spectra, which reveal a strong band at  $969\text{ cm}^{-1}$  for [VO(salhyhb)(hq)] and  $972\text{ cm}^{-1}$  for [VO(salhyhp)(hq)] and [VO(salhyhh)(hq)], characteristic of the stretching vibration of the V=O moiety. Moreover, upon complex formation the bands that are characteristic of the N–H and C=O stretching vibrations of the ligand disappear in the IR spectra and a new strong band shows up at around  $1605\text{ cm}^{-1}$ , which is typical for the conjugated  $-\text{CH}=\text{N}-\text{N}=\text{C}-$  system with the *N'*-salicylidenehydrazide ligand present in its enolate form.<sup>[23]</sup> A broad band attributed to the O–H stretching vibration of the hydroxy group of the side chain is observed at around  $3440\text{ cm}^{-1}$ . Further evidence for the complexation of the coligand is given by the presence of its characteristic

aromatic C–C stretching vibrations together with the disappearance of the  $\nu(\text{OH})$  vibration of the free 8-hydroxyquinoline at  $3152\text{ cm}^{-1}$ .

For all complexes synthesized, strong bands are observed in the electronic absorption spectra of their acetonitrile solutions at 241, 273, 321, and 540 nm. In comparison with the electronic spectra of the corresponding free ligands an additional band is apparent in the visible region at 540 nm ( $\epsilon \approx 7000\text{ cm}^{-1}\text{ M}^{-1}$ ), which is attributed to a ligand-to-metal charge-transfer band.

The  $^1\text{H}$  and  $^{13}\text{C}$  NMR spectroscopic data for all complexes are consistent with the formation of the proposed mixed-ligand oxidovanadium(V) complexes. In particular, the twofold deprotonation of the *N'*-salicylidenehydrazide ligands is evident from the absence of the downfield resonances corresponding to the O–H and N–H protons in the  $^1\text{H}$  NMR spectra of the complexes. Moreover, upon coordination the resonance of the azomethine proton is shifted downfield to 9.15 ppm, whereas the resonances of the hydrogen atoms of the methylene group next to the carbonyl group are slightly shifted upfield when the vanadium atom is coordinated. The  $^{13}\text{C}$  NMR spectroscopic data confirm the simultaneous coordination of both chelate ligands, the Schiff base, and the 8-hydroxyquinoline coligand.

The  $^{51}\text{V}$  NMR spectra confirm the presence of one species for solutions of the complexes in DMSO and chloroform with observed resonances at  $-472$  and  $-483$  ppm, respectively. This indicates a considerable solvent dependence for the  $^{51}\text{V}$  NMR resonances of the mixed-ligand complexes. The observed hydrolytic stability of these complexes in DMSO/water mixtures is consistent with the described pronounced stability of phenolate substituted oxidovanadium(V) complexes.<sup>[10]</sup> Nevertheless, they can be converted into the corresponding *cis*-dioxidovanadium(V) complexes by treatment with an aqueous sodium hydroxide solution. Monitoring this reaction by  $^{51}\text{V}$  NMR spectroscopy shows that 1 equiv. of alkaline base is required for a complete cleavage of the 8-hydroxyquinolinato coligand, with a resonance at  $-536$  ppm for the final *cis*-dioxidovanadium(V) complex<sup>[28]</sup> that is stable even in the presence of excess base.

### Electrochemical Properties

The electrochemical properties of the complexes [VO(hq)(salhyhb)], [VO(hq)(salhyhp)], and [VO(hq)(salhyhh)] in acetonitrile solutions have been investigated by cyclic square-wave voltammetry. As all three complexes exhibit a similar electrochemical behavior, a typical series of cyclic square-wave voltammograms measured for [VO(hq)(salhyhp)] with square-wave frequencies ranging from 25 to 1500 Hz is depicted in Figure 1. The two observed one-electron reduction steps correspond to the reactions shown in Equation (1) and Equation (2).



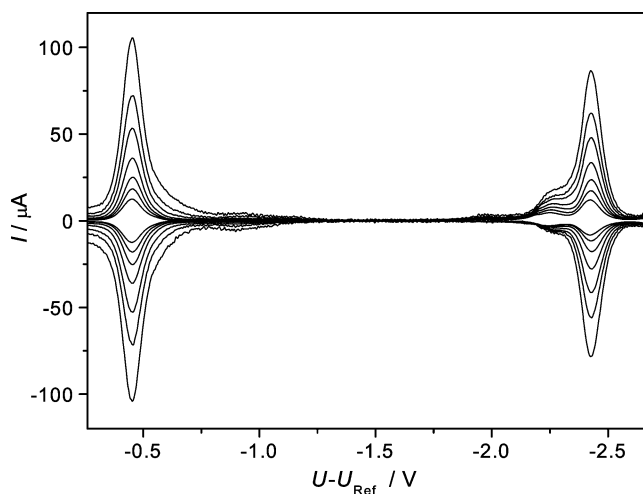


Figure 1. Square-wave voltammograms of complex  $[\text{VO}(\text{salhyhb})(\text{hq})]$  in acetonitrile with applied square-wave frequencies of 25, 50, 100, 200, 400, 800, and 1500 Hz (with increasing peak current).

The first reduction step, which occurs at a half-wave potential of  $U_1^{1/2} = -0.452$  V, appears to be fully reversible for square-wave frequencies up to 1500 Hz, whereas the second reduction step at a potential of  $U_2^{1/2} = -2.428$  V is accompanied by a pre-wave. These electrochemical features are basically similar to what has been observed for mixed-ligand oxidovanadium(V) complexes based on non-functionalized *N'*-salicylidenehydrazide ligands,<sup>[35]</sup> although the two half-wave potentials for the latter cases are somewhat shifted to more negative values ( $U_1^{1/2} = -0.460$  V and  $U_2^{1/2} = -2.453$  V).

The frequency dependence of the peak current of the reduction steps related to Equation (1) and (2) as well as that of the accompanying pre-wave of the second step is depicted in Figure 2. This shows that the first reduction step is diffusion controlled over the entire frequency range. For the second reduction step the peak current shows a similar behavior and stays at least close to this limit, whereas its accompanying pre-wave reaches a steady-state current for very high square-wave frequencies. Even for low square-wave frequencies this peak current deviates significantly from the diffusion controlled limit, indicating that this pre-wave is associated with the reduction of a species generated by a preceding chemical equilibrium. Species potentially responsible for the observed pre-wave feature are the 8-hydroxyquinolate anion  $\text{hq}^-$  and the deprotonated  $\text{Hsalhyhp}^-$  ligand with reversible one-electron reduction processes at potentials of about  $-2.33$  V and  $-2.10$  V, respectively. Given the potential range observed for the pre-wave we prefer an interpretation based on the 8-hydroxyquinolate anion  $\text{hq}^-$  [Equation (3)].



In order to sufficiently describe the observed data a complex system of addition/elimination reactions given in Equations (4) and (5) together with the corresponding

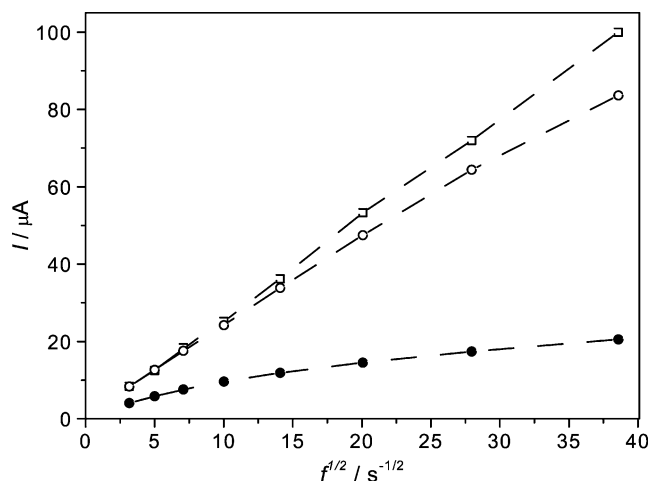
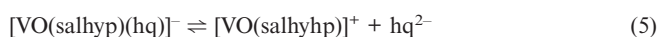
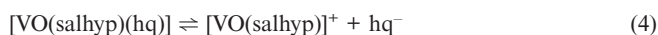


Figure 2. Height of the peak current for the first (open squares) and the second reduction step (open circles) as well as the plateau current of the pre-wave (filled circles) associated with the second reduction step of complex  $[\text{VO}(\text{salhyhb})(\text{hq})]$  as a function of the square root of the square-wave frequency.

charge transfer reactions given in Equations (1) to (3) is necessary. This is also required for the underlying reaction scheme to satisfy the condition of an early diffusion controlled peak current for the second reduction step, excluding the option of a single chemical equilibrium linking the product of the first reduction step with the species responsible for the pre-wave feature. Moreover, this is corroborated by the observed frequency-dependent shift of the pre-wave towards more positive potentials for a decrease in the square-wave frequency (see Figure 1), which is exactly the opposite shift theoretically expected for a simple pre-equilibrium.



The simulation of the electrochemical data is depicted in Figure 3, showing a reasonable agreement with the experimental data based on the assumed addition/elimination reactions given in Equation (4) and (5) for the vanadium(V) complex and its singly reduced vanadium(IV) analog generated according to Equation (1), respectively. The equilibria given in Equation (4) and (5) are found to be far on the side of the intact complexes. Nevertheless, for potentials between the first reduction step and the pre-wave the equilibrium in Equation (5) is somewhat shifted to the side of the dissociated products, as even small amounts of  $\text{hq}^{2-}$  are instantly reoxidized to  $\text{hq}^-$ . Together with Equation (4) this can account for the virtually diffusion-controlled behavior of the second reduction step, simply by regeneration of the corresponding  $[\text{VO}(\text{salhy})\text{(hq)}]^-$  species. Consequently, the difference in the equilibrium constants for the reactions given in Equation (4) and (5) results in the accumulation of effects leading to the generation of a pre-wave for the second reduction step. In addition, this can also account for the unusual frequency dependence of the potential shift of

this pre-wave as well as the observed virtual diffusion control of the peak current of the second reduction step. It should be mentioned here that basically similar and/or additional effects could be expected from appropriate differences in the diffusion coefficients of the underlying species. Nevertheless, for practicability reasons this has not been included in the present simulations.

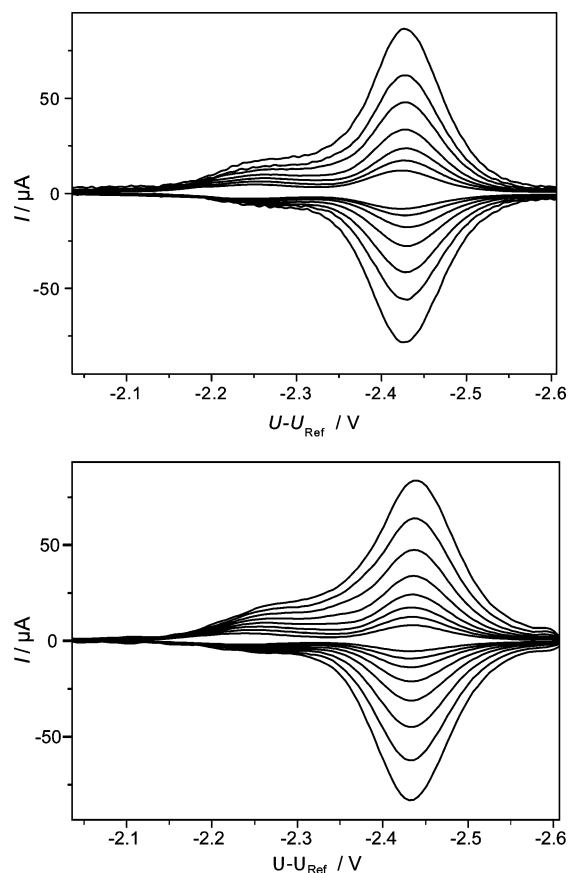


Figure 3. Measured (top) and simulated (bottom) square-wave voltammograms of complex  $[\text{VO}(\text{salhyhb})(\text{hq})]$  in acetonitrile with applied square-wave frequencies of 25, 50, 100, 200, 400, 800, and 1500 Hz (with increasing peak current).

### Structure of $[\text{VO}(\text{hq})(\text{salhyhb})]$

Crystals suitable for X-ray diffraction could be isolated for complex  $[\text{VO}(\text{hq})(\text{salhyhb})]$  by crystallization from a methanol/acetonitrile (1:1) mixture upon slow evaporation of the solvents at room temperature. The complex crystallizes in the triclinic space group  $P\bar{1}$  with two crystallographically independent molecules in the asymmetric unit. The molecular structures are depicted in Figure 4 and selected bond lengths and angles are given in Table 1.

In both independent molecules of  $[\text{VO}(\text{hq})(\text{salhyhb})]$  the vanadium atom is six-coordinate in a distorted-octahedral geometry with similar structural features. The  $N'$ -salicylidenehydrazide ligand is fully deprotonated and acts as a tridentate-chelate system coordinating through its ONO donor set (O12, N11, O13 or O22, N21, O23), which together with the oxygen atom of the bidentate 8-hydroxyquinoline

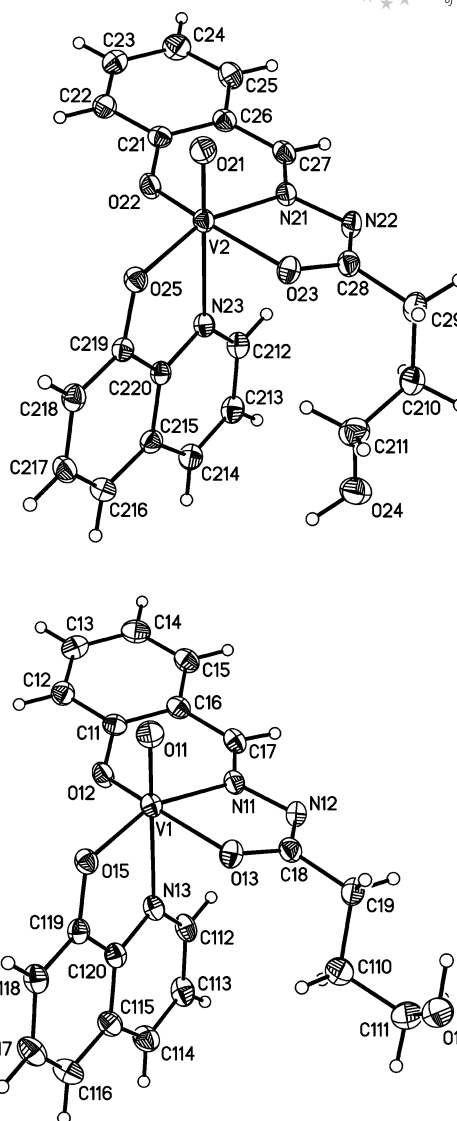


Figure 4. Molecular structures of the two independent complexes in the crystal structure of  $[\text{VO}(\text{salhyhb})(\text{hq})]$ . Thermal ellipsoids of non-hydrogen atoms are drawn at the 50% probability level.

ligand (O15 or O25) forms a tetragonal basal plane. Five- and a six-membered-chelate rings are established by the hydrazone ligand with bite angles of  $75^\circ$  (O13–V1–N11, O23–V2–N21) and  $84^\circ$  (O12–V1–N11, O22–V2–N21), respectively. The V=O moiety in both molecules shows a bond length of about 159 pm, which is at the lower end of the typically observed range for  $\text{VO}^{3+}$  complexes,<sup>[9–12]</sup> but consistent with other complexes containing hydrazone ligands together with appropriate coligands such as 8-hydroxyquinoline,<sup>[36]</sup> catechol,<sup>[37]</sup> hydroxamate,<sup>[38,39]</sup> and polyols.<sup>[40]</sup> The *trans* influence of the oxido group leads to a rather long V–N bond to the nitrogen atom of the 8-hydroxyquinoline coligand (235 pm), and consequently to a displacement of the vanadium atom towards the oxido group out of the tetragonal basal plane by about 30 pm. The observed bond lengths of the amide group of the hydrazone ligand are consistent with its dianionic form,<sup>[23,28]</sup> whereas for complexes

Table 1. Selected bond lengths [pm] and angles [°] for [VO(salhyhb)(hq)].

Distances			
V1–O11	159.38(15)	V2–O21	159.79(14)
V1–O12	186.09(14)	V2–O22	185.04(14)
V1–O13	195.77(14)	V2–O23	195.09(14)
V1–O15	184.28(14)	V2–O25	184.97(14)
V1–N11	207.89(17)	V2–N21	207.91(17)
V1–N13	235.44(17)	V2–N23	235.35(16)
O13–C18	130.8(2)	O23–C28	131.3(2)
N12–C18	130.3(3)	N22–C28	130.1(3)
Angles			
O11–V1–O12	98.88(7)	O21–V2–O22	99.59(7)
O11–V1–O13	99.02(7)	O21–V2–O23	97.04(7)
O11–V1–O15	101.26(7)	O21–V2–O25	99.21(7)
O11–V1–N11	98.05(7)	O21–V2–N21	99.95(7)
O11–V1–N13	176.51(7)	O21–V2–N23	173.81(7)
O12–V1–O13	153.98(6)	O22–V2–O23	155.27(6)
O12–V1–O15	103.33(6)	O22–V2–O25	101.34(6)
O12–V1–N11	83.83(6)	O22–V2–N21	83.79(6)
O12–V1–N13	84.26(6)	O22–V2–N23	85.47(6)
O13–V1–O15	91.50(6)	O23–V2–O25	93.89(6)
O13–V1–N11	75.09(6)	O23–V2–N21	75.37(6)
O13–V1–N13	78.51(6)	O23–V2–N23	79.33(6)
O15–V1–N11	158.01(6)	O25–V2–N21	159.03(6)
O15–V1–N13	76.46(6)	O25–V2–N23	76.18(6)
N11–V1–N13	83.73(6)	N21–V2–N23	84.05(6)

with the coordinated keto form of the ligand the C–O bond is considerably elongated.<sup>[22]</sup>

The hydrogen-bonding interactions induced by the hydroxy group of the side-chain substituted *N'*-salicylidenehydrazide ligand leads to the formation of a chainlike arrangement as depicted in Figure 5. The different roles of the two crystallographically independent molecules within this chain define their structural differences. Basically this chain is formed by the molecules containing the vanadium atom V2 with a hydrogen-bonding relay between the oxido group O21 and the hydroxy group O24 from an adjacent molecule of the same type. The hydrogen-bonding relay is established by the hydroxy group (O14) of the other crystallographically unique molecules (V1) present in the structure, which form tails sticking out on one side of the chain core. This difference between the two independent molecules also reflects in their molecular structure such that

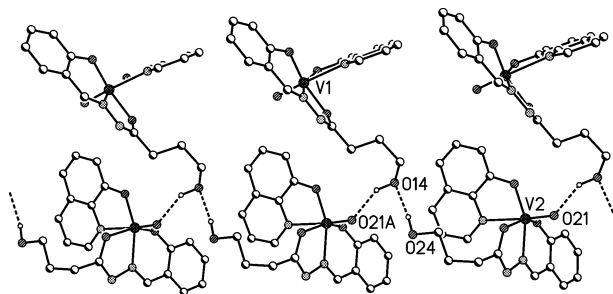


Figure 5. Representation of the hydrogen bonding interactions between the two independent molecules of [VO(salhyhb)(hq)] leading to chains along the *a* axis; hydrogen atoms attached to carbon atoms are omitted for clarity; broken lines represent hydrogen bonds; relevant distances (in pm): O14...O24 286, O14...O21A 288.

their pendant side chains possess different orientations given by the  $Ci8-Ci9-Ci10-Ci11$  torsion angles ( $172^\circ$  for  $i = 1$ ,  $-68^\circ$  for  $i = 2$ ).

These chains associate in the solid state by  $\pi$ - $\pi$ -stacking interactions of the 8-hydroxyquinoline coligands from both types of molecules present. This stacking occurs in such a fashion that an alternating pairwise core-to-core [V2(hq)⋯(hq)V2] and tail-to-tail [V1(hq)⋯(hq)V1] interaction of adjacent chains is observed leading to a two-dimensional array within the crystallographic (01 $\bar{1}$ ) plane. Figure 6 shows the resultant packing with the view approximately along the hydrogen-bonded chains.

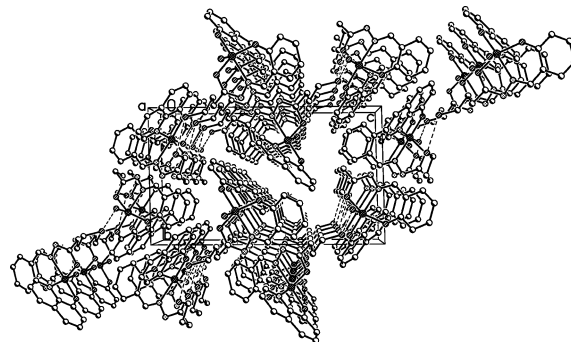


Figure 6. Packing diagram for [VO(salhyhb)(hq)] (view approximately down the *a* axis).

### <sup>51</sup>V MAS NMR Spectroscopy

<sup>51</sup>V NMR spectra of the complexes [VO(hq)(salhyhb)], [VO(hq)(salhyhp)], and [VO(hq)(salhyhh)] as well as of their analogs with the hydroxy-free side chain [VO(hq)(salhyb)],

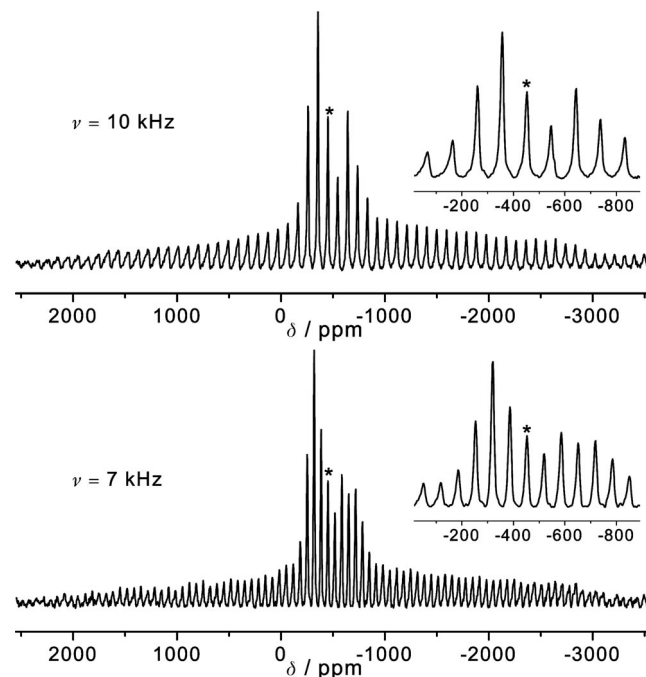


Figure 7. <sup>51</sup>V solid-state MAS NMR spectra of [VO(salhyhp)(hq)] measured at 9.4 T and spinning rates of 7 kHz (bottom) and 10 kHz (top). Insets show an expansion of the central transition region.

[VO(hq)(salhyp)], and [VO(hq)(salhyh)] were measured at 9.4 T applying different rates for the magic-angle spinning. In Figure 7 the experimental spectra acquired for [VO(hq)(salhyhp)] with spinning rates of 7 and 10 kHz are depicted. The comparison of spectra, measured at different spinning rates, enables the unambiguous determination of the observable isotropic peak ( $\delta_{\text{obsd}}$ ). In addition, this increases the reliability of the parameters determined by numerical simulations, the latter being essential for a quadrupolar nucleus like  $^{51}\text{V}$  ( $I = 7/2$ ).

The experimental  $^{51}\text{V}$  magic-angle spinning NMR spectra of the examined complexes are depicted in Figure 8 and the determined spectral parameters are listed in Table 2. Because of the second-order quadrupole induced shift, the observed isotropic shift  $\delta_{\text{obsd}}$  is corrected according to Equation (6)<sup>[41]</sup>

$$\delta_{\text{obsd}} - \delta_{\text{iso}} = -3 \cdot 10^6 \left( \frac{e^2 q Q}{h} \right)^2 \frac{[I(I+1) - 9m(m-1) - 3][1 + \eta_Q^2/3]}{40\nu_0^2 [I(2I-1)]^2} \quad (6)$$

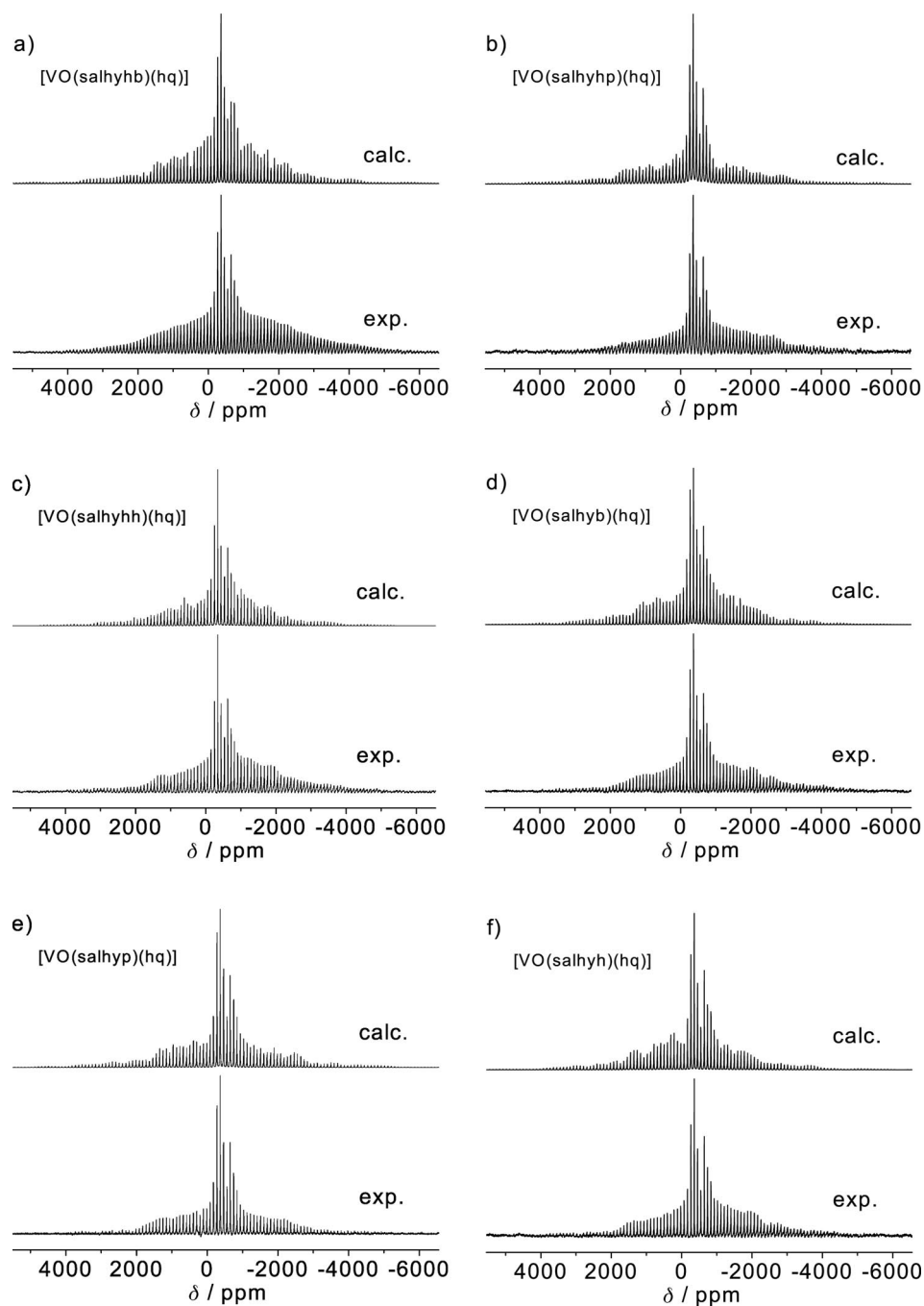


Figure 8.  $^{51}\text{V}$  solid-state MAS NMR spectra of (a) [VO(salhyhb)(hq)], (b) [VO(salhyhp)(hq)], (c) [VO(salhyhh)(hq)], (d) [VO(salhyb)(hq)], (e) [VO(salhyp)(hq)], and (f) [VO(salhyh)(hq)] measured at 9.4 T and a spinning rate of 10 kHz. The calculated spectra were obtained with the parameters summarized in Table 2.

Table 2. Solid-state NMR parameters for mixed-ligand oxidovanadium(V) complexes.<sup>[a]</sup>

	$C_Q$ [MHz]	$\eta_Q$	$\delta_\sigma$ [ppm]	$\eta_\sigma$	$\delta_{\text{obsd}}$ [ppm]	Quadrupole induced shift <sup>[b]</sup> [ppm]	$\delta_{\text{iso}}$ [ppm]	$\delta_{\text{iso}}(\text{solution})$ [ppm]
[VO(salhyhb)(hq)]	4.0	0.4	-449	0.4	-454.2	-3.9	-450.1	-472
[VO(salhyhp)(hq)]	4.3	0.8	-409	0.3	-452.3	-5.2	-446.7	-472
[VO(salhyhh)(hq)]	3.5	0.6	-407	0.3	-436.7	-3.2	-433.1	-472
[VO(salhyb)(hq)]	3.5	0.7	-431	0.4	-461.7	-3.3	-458.4	-472
[VO(salhyp)(hq)]	3.8	0.8	-436	0.2	-463.9	-4.0	-460.1	-472
[VO(salhyh)(hq)]	3.5	0.6	-438	0.2	-454.0	-3.2	-450.6	-472

[a] Quadrupolar couplings ( $C_Q$ ,  $\eta_Q$ ), chemical shift anisotropies ( $\delta_\sigma$ ,  $\eta_\sigma$ ), and the  $^{51}\text{V}$  chemical shifts ( $\delta_{\text{obsd}}$ ,  $\delta_{\text{iso}}$ ); for details see Exp. Sect.; the following error margins apply:  $C_Q \pm 0.2$  MHz,  $\eta_Q \pm 0.1$ ,  $\delta_\sigma \pm 20$  ppm,  $\eta_\sigma \pm 0.1$ ,  $\delta_{\text{obsd}} \pm 3$  ppm,  $\delta_{\text{iso}} \pm 1$  ppm. [b] Calculated according to Equation (6).

where ( $e^2qQ/h$ ) is the nuclear quadrupolar coupling constant  $C_Q$  given in MHz,  $I$  is the spin number ( $I = 7/2$  for  $^{51}\text{V}$ ),  $m$  is the magnetic spin number ( $m = 1/2$  for the central transition),  $\eta_Q$  is the asymmetry of the EFG tensor, and  $\nu_0$  the resonance frequency of the  $^{51}\text{V}$  nucleus (105.19 MHz at 9.4 T). As can be seen from Table 2 this second-order correction is found to be within  $-3$  and  $-5$  ppm. This is because of the comparatively small values of the nuclear quadrupolar coupling constant in the order of about 4 MHz, which is at the lower end of the usually observed range for oxidovanadium(V)<sup>[42,43]</sup> and dioxidovanadium(V)<sup>[44]</sup> complexes going up to about 7 MHz. Nevertheless, the spectra are characterized by a considerable asymmetry of the EFG tensor with values between 0.4 and 0.8. The determined nuclear quadrupolar coupling constants  $C_Q$  and asymmetry parameters  $\eta_Q$  of the EFG tensor are related to the overall width and shape, respectively, of the spectra given in Figure 8.

The NMR parameters given in Table 2 show a significant variation for the series of complexes under investigation, although the differences in geometry of the first coordination sphere of the vanadium centers for the structurally characterized vanadium(V) complexes (see Table 1 and ref.<sup>[35]</sup>) are very small (bond lengths  $< 2$  pm; bond angles  $< 5^\circ$ ). In addition, for all complexes large discrepancies have been observed between the isotropic chemical shifts in the solid state and in solution, which ranges from about 10 to 40 ppm. It is tempting to attribute this to a high sensitivity of the chemical-shielding interaction at the vanadium nucleus with respect to changes in the local environment. However, this can only be attributed to subtle differences introduced through secondary coordination effects, e.g. hydrogen bonding (see Figure 5) or crystal packing, caused by a variation of the side chain.

Consequently, the solution chemical shifts are the same for all six complexes in a given solvent, despite their actual side-chain characteristics. This can be rationalized in terms of the solvent molecules interacting with the complexes in a similar fashion. Moreover, in solution the side chains can be expected to freely relax their orientation away from the vanadium center, which leads to a separation of the side-chain functionality preventing any kind of interference with the vanadium atom. It is interesting to note that even changing the solvent environment from DMSO to chloro-

form induces an additional shielding effect of about 10 ppm and that this solvent induced difference is in the same order of magnitude as the observed variation of the isotropic chemical shift values in the solid state ( $\delta = 27$  ppm).

The anisotropy parameter  $\delta_\sigma$  of the chemical-shielding anisotropy (CSA) tensor for the three complexes with the alkyl side chains are within 7 ppm indicating rather subtle differences in the chemical environment, which is consistent with their observed structural similarities.<sup>[35]</sup> Somewhat larger effects are observed for the hydroxyl-functionalized side chains with an observed range of about 40 ppm (see Table 1). Interestingly, the two complexes [VO(salhyhp)(hq)] and [VO(salhyhh)(hq)] exhibit a value of  $\delta = -408$  ppm about the same anisotropy, whereas for the complex with the shortest alkyl spacer [VO(salhyhb)(hq)] a value of  $\delta = -449$  ppm is observed. Unfortunately, we could not obtain suitable crystals of the former two complexes to better elucidate possible structural correlations. Nevertheless, this could suggest a variation in the hydrogen bonding, as an elongation of the alkyl spacer might prevent the analogous assembly in the solid state.

Finally, the observed rather low asymmetry of the CSA tensor ( $\eta_Q$  in Table 2), which is in the range of 0.2 to 0.4, is consistent with a predominant role of the V=O bond for determining the magnetic shielding at the vanadium(V) center. The strong influence of the V=O bond is in agreement with earlier reports on magnetic-shielding effects on chelate rings in oxidovanadium(V) complexes, which indicate a strong anisotropy around this functional group.<sup>[11]</sup>

## Conclusions

Mixed-ligand oxidovanadium(V) complexes containing hydroxyl-functionalized *N'*-salicylidenehydrazides and 8-hydroxyquinoline have been synthesized. These complexes exhibit an electrochemistry with two one-electron reduction steps, which can only be explained on the basis of a coupled reaction system including addition/elimination reactions of the 8-hydroxyquinoline ligand with regard to the vanadium(V) and the corresponding reduced vanadium(IV) complexes. The crystal structure of complex [VO(salhyhb)(hq)] reveals hydrogen-bonding interactions of the side chain of one molecule with the oxido group of an adjacent indepen-

dent second complex molecule. This supramolecular differentiation does not lead to a significant alteration of the structural parameters of the two crystallographically independent molecules. This also reflects in the measured solid-state MAS NMR spectra, which do not allow a differentiation of these two vanadium nuclei. Nevertheless, these NMR spectra indicate an influence of the crystal environment on the EFG and CSA tensors, which is only somewhat larger than the observed solvent induced changes for the isotropic chemical shift. Nevertheless, the CSA tensor is very sensitive towards changes in the local environment of vanadium(V) nuclei and in the presence of an oxido group dominated by the V=O bond.

## Experimental Section

**Materials:** Abbreviations used throughout the text: H<sub>2</sub>salhyb = *N'*-(2-hydroxyphenyl)methylidene]butanohydrazide, H<sub>2</sub>salhyp = *N'*-(2-hydroxyphenyl)methylidene]pentanohydrazide, H<sub>2</sub>salhyh = *N'*-(2-hydroxyphenyl)methylidene]hexanohydrazide, H<sub>2</sub>salhyhb = 4-hydroxy-*N'*-(2-hydroxyphenyl)methylidene]butanohydrazide, H<sub>2</sub>salhyhp = 5-hydroxy-*N'*-(2-hydroxyphenyl)methylidene]pentanohydrazide, H<sub>2</sub>salhyhh = 6-hydroxy-*N'*-(2-hydroxyphenyl)methylidene]hexanohydrazide, Hhq = 8-hydroxyquinoline. The ω-hydroxycarbohydrazides were prepared by the treatment of the corresponding lactone with 2 equiv. hydrazine hydrate and have been recrystallized from absolute ethanol. The complexes [VO(salhyb)(hq)], [VO(salhyp)(hq)], and [VO(salhyh)(hq)] have been prepared according to reported procedures.<sup>[35]</sup> All other reagents were used as received without further purification.

**Instrumentation:** Solution <sup>1</sup>H, <sup>13</sup>C, <sup>51</sup>V, <sup>1</sup>H{<sup>1</sup>H} COSY, and <sup>1</sup>H{<sup>13</sup>C} heteronuclear correlation NMR spectra were recorded with Bruker AVANCE 200 and 400 MHz spectrometers. IR spectra were measured with a Bruker IFS55/Equinox spectrometer on samples prepared as KBr pellets. Elemental analysis (C, H, N) were determined with Leco CHNS-932 and El Vario III elemental analyzers. UV/Vis spectra were recorded with a Varian Cary 5000 UV/Vis/NIR spectrophotometer using spectral grade acetonitrile.

**Synthesis of ω-Hydroxy-*N'*-salicylidenehydrazides:** Salicylaldehyde (1 equiv.) was added dropwise to a solution of the ω-hydroxycarbohydrazide (about 40 mmol) in methanol (100 mL) under continuous stirring at room temperature. The resulting solution was stirred at room temperature for an additional 12 h. The colorless precipitate that formed was separated by filtration. Additional material can be obtained from the remaining solution by removal of the solvent under reduced pressure.

**H<sub>2</sub>salhyhb:** 4-Hydroxybutanohydrazide (5.00 g, 42 mmol) and salicylaldehyde (5.17 g, 42 mmol). Yield 8.30 g (37 mmol, 88%). C<sub>11</sub>H<sub>14</sub>N<sub>2</sub>O<sub>3</sub> (222.24): calcd. C 59.45, H 6.35, N 12.61; found C 59.40, H 6.50, N 12.58. M.p. 122–123 °C. <sup>1</sup>H NMR (200 MHz, [D<sub>6</sub>]-DMSO): δ = 1.71 (tt, <sup>3</sup>J<sub>av</sub> = 6.9 Hz, 2 H, CH<sub>2</sub>CH<sub>2</sub>OH), 2.25 and 2.60 (both t, <sup>3</sup>J = 7.5 Hz, total 2 H, CH<sub>2</sub>C=O), 3.37–3.47 (m, 2 H, CH<sub>2</sub>OH), 4.49–4.58 (m, 1 H, CH<sub>2</sub>OH), 6.85–6.91 (m, 2 H, arom. CH), 7.22–7.26 (m, 1 H, arom. CH), 7.44–7.60 (m, 1 H, arom. CH), 8.24 and 8.32 (both s, total 1 H, CH=N), 10.15, 11.20, 11.60 (all s, total 2 H, NH and OH) ppm. Selected IR data (KBr):  $\tilde{\nu}$  = 3185 (s, NH, OH<sub>ass</sub>), 1673 (s, C=O), 1623 (s, CH=N) cm<sup>-1</sup>. UV/Vis (CH<sub>3</sub>CN solution): λ<sub>max</sub> (ε) = 278 (16,400), 288 (14,900), 319 nm (7700 cm<sup>-1</sup>M<sup>-1</sup>).

**H<sub>2</sub>salhyhp:** 5-Hydroxypentanohydrazide (5.24 g, 43 mmol) and salicylaldehyde (5.67 g, 43 mmol). Yield 9.67 g (41 mmol, 95%).

C<sub>12</sub>H<sub>16</sub>N<sub>2</sub>O<sub>3</sub> (236.27): calcd. C 61.00, H 6.83, N 11.86; found C 60.92, H 6.82, N 11.74. M.p. 122–123 °C. <sup>1</sup>H NMR (200 MHz, [D<sub>6</sub>]-DMSO): δ = 1.40–1.49 (m, 2 H, CH<sub>2</sub>CH<sub>2</sub>OH), 1.56–1.63 (m, 2 H, CH<sub>2</sub>CH<sub>2</sub>C=O), 2.36 and 2.57 (both t, <sup>3</sup>J = 7.5 Hz, total 2 H, CH<sub>2</sub>C=O), 3.37–3.42 (m, 2 H, CH<sub>2</sub>OH), 4.38–4.42 (m, 1 H, CH<sub>2</sub>OH), 6.83–6.90 (m, 2 H, arom. CH), 7.19–7.27 (m, 1 H, arom. CH), 7.46–7.61 (m, 1 H, arom. CH), 8.24 and 8.33 (both s, total 1 H, CH=N), 10.13, 11.20, 11.57 (all s, total 2 H, NH and OH) ppm. Selected IR data (KBr):  $\tilde{\nu}$  = 3185 (s, NH, OH<sub>ass</sub>), 1673 (s, C=O), 1623 (s, CH=N) cm<sup>-1</sup>. UV/Vis (CH<sub>3</sub>CN solution): λ<sub>max</sub> (ε) = 278 (16,600), 288 (14,800), 319 nm (7800 cm<sup>-1</sup>M<sup>-1</sup>).

**H<sub>2</sub>salhyhh:** 6-Hydroxyhexanohydrazide (5.00 g, 34 mmol) and salicylaldehyde (4.18 g, 34 mmol). Yield 7.10 g (28 mmol, 82%). C<sub>13</sub>H<sub>18</sub>N<sub>2</sub>O<sub>3</sub> (250.30): calcd. C 62.38, H 7.25, N 11.19; found C 62.38, H 7.28, N 11.23. M.p. 130–131 °C. <sup>1</sup>H NMR (200 MHz, [D<sub>6</sub>]-DMSO): δ = 1.23–1.47 (m, 4 H, CH<sub>2</sub>CH<sub>2</sub>CH<sub>2</sub>OH), 1.57 (tt, <sup>3</sup>J<sub>av</sub> = 7.3 Hz, 2 H, CH<sub>2</sub>CH<sub>2</sub>C=O), 2.20 and 2.56 (both t, <sup>3</sup>J = 7.5 Hz, total 2 H, CH<sub>2</sub>C=O), 3.34–3.41 (m, 2 H, CH<sub>2</sub>OH), 4.37 (br. s, 1 H, CH<sub>2</sub>OH), 6.85–6.91 (m, 2 H, arom. CH), 7.21–7.30 (m, 1 H, arom. CH), 7.44–7.60 (m, 1 H, arom. CH), 8.24 and 8.32 (both s, total 1 H, CH=N), 10.13, 11.19, 11.58 (all s, total 2 H, NH and OH) ppm. Selected IR data (KBr):  $\tilde{\nu}$  = 3185 (s, NH, OH<sub>ass</sub>), 1673 (s, C=O), 1623 (s, CH=N) cm<sup>-1</sup>. UV/Vis (CH<sub>3</sub>CN solution): λ<sub>max</sub> (ε) = 278 (16,300), 288 (15,000), 319 nm (7500 cm<sup>-1</sup>M<sup>-1</sup>).

**Synthesis of Vanadium Complexes:** The appropriate ω-hydroxy hydrazide ligand (2 mmol) was dissolved in methanol (25 mL) and added to a stirred suspension of [VO(acac)<sub>2</sub>] (0.53 g, 2 mmol) in methanol (10 mL). The resulting reaction mixture was heated under reflux for 2 h with continuous stirring. The color changed from green to brown. Over a period of 30 min a solution of 8-hydroxyquinoline (0.29 g, 2 mmol) in methanol (10 mL) was added dropwise and the stirred reaction solution was heated under reflux for an additional 2 h. This reaction scheme can also be performed in acetonitrile, which generally leads to somewhat better yields. The solvent was removed to dryness under reduced pressure and the residue recrystallized from a mixture of methanol and acetonitrile (1:1), which yielded dark violet needles.

**[VO(salhyhb)(hq)]:** Yield 0.57 g (1.3 mmol, 65%) in methanol and 0.63 g (1.4 mmol, 70%) in acetonitrile. C<sub>20</sub>H<sub>18</sub>N<sub>3</sub>O<sub>5</sub>V (443.40): calcd. C 56.69, H 4.21, N 9.74; found C 56.29, H 4.26, N 9.92. <sup>1</sup>H NMR (400 MHz, [D<sub>6</sub>]DMSO): δ = 1.26 (tt, <sup>3</sup>J<sub>av</sub> = 7.0 Hz, 2 H, CH<sub>2</sub>CH<sub>2</sub>OH), 2.09 (t, 2 H, <sup>3</sup>J = 7.4 Hz, CH<sub>2</sub>C=O), 3.09 (t, 2 H, <sup>3</sup>J = 6.4 Hz, CH<sub>2</sub>OH), 4.26 (br. s, 1 H, OH), 6.72–6.74 (m, 1 H, arom. CH), 6.98–7.00 (m, 1 H, arom. CH), 7.17–7.18 (m, 1 H, arom. CH), 7.45–7.80 (m, 5 H, arom. CH), 8.09–8.10 (m, 1 H, arom. CH), 8.50–8.52 (m, 1 H, arom. CH), 9.14 (s, 1 H, CH=N) ppm. <sup>13</sup>C NMR (100 MHz, [D<sub>6</sub>]DMSO): δ = 26.3 (CH<sub>2</sub>CH<sub>2</sub>OH), 29.1 (CH<sub>2</sub>C=O), 59.6 (CH<sub>2</sub>OH), 110.9, 115.4, 119.5, 120.4, 122.5, 123.0, 128.2, 129.0, 133.2, 135.2, 138.2, 138.5, 146.1 (all arom. CH and C), 154.2 (CH=N), 162.3, 163.3 (both arom. CO-V), 176.1 (CO-V) ppm. <sup>51</sup>V NMR (105 MHz, [D<sub>6</sub>]-DMSO): δ = -472 ppm (Δ<sub>v1/2</sub> = 358 Hz). <sup>51</sup>V NMR (105 MHz, CDCl<sub>3</sub>): δ = -483 ppm (Δ<sub>v1/2</sub> = 148 Hz). Selected IR data (KBr):  $\tilde{\nu}$  = 3446 (br., O-H), 1605 (s, CH=N-N=C), 969 (s, V=O) cm<sup>-1</sup>. UV/Vis (CH<sub>3</sub>CN solution): λ<sub>max</sub> (ε) = 241 (43,500), 273 (20,800), 321 (9100), 540 nm (6800 cm<sup>-1</sup>M<sup>-1</sup>).

**[VO(salhyhp)(hq)]:** Yield 0.45 g (1.0 mmol, 50%) in methanol and 0.69 g (1.6 mmol, 80%) in acetonitrile. C<sub>21</sub>H<sub>20</sub>N<sub>3</sub>O<sub>5</sub>V (445.35): calcd. C 56.64, H 4.53, N 9.44; found C 57.00, H 4.43, N 8.97. <sup>1</sup>H NMR (400 MHz, [D<sub>6</sub>]DMSO): δ = 1.04–1.17 (m, 4 H, CH<sub>2</sub>CH<sub>2</sub>CH<sub>2</sub>OH), 2.07 (t, 2 H, <sup>3</sup>J = 6.6 Hz, CH<sub>2</sub>C=O), 3.09 (t, 2 H, CH<sub>2</sub>OH, <sup>3</sup>J = 6.4 Hz), 4.21 (br. s, 1 H, OH), 6.72–6.76 (m, 1

H, arom. CH), 6.97–7.04 (m, 1 H, arom. CH), 7.16–7.21 (m, 1 H, arom. CH), 7.45–7.50 (m, 1 H, arom. CH), 7.55–7.60 (m, 1 H, arom. CH), 7.70–7.73 (m, 2 H, arom. CH), 7.79–7.82 (m, 1 H, arom. CH), 8.08–8.11 (m, 1 H, arom. CH), 8.50–8.54 (m, 1 H, arom. CH), 9.15 (s, 1 H, CH=N) ppm.  $^{13}\text{C}$  NMR (50 MHz,  $[\text{D}_6]\text{-DMSO}$ ):  $\delta = 22.3$  ( $\text{CH}_2\text{CH}_2\text{C}=\text{O}$ ), 29.2 ( $\text{CH}_2\text{C}=\text{O}$ ), 31.3 ( $\text{CH}_2\text{CH}_2\text{OH}$ ), 59.9 ( $\text{CH}_2\text{OH}$ ), 110.8, 115.4, 119.4, 120.4, 122.5, 123.0, 128.2, 129.0, 133.2, 135.2, 138.3, 138.5, 146.2 (all arom. CH and C), 154.2 (CH=N), 162.3, 163.2 (both arom. CO–V), 176.0 (CO–V) ppm.  $^{51}\text{V}$  NMR (105 MHz,  $[\text{D}_6]\text{-DMSO}$ ):  $\delta = -472$  ppm ( $\Delta\nu_{1/2} = 357$  Hz).  $^{51}\text{V}$  NMR (105 MHz,  $\text{CDCl}_3$ ):  $\delta = -483$  ppm ( $\Delta\nu_{1/2} = 148$  Hz). Selected IR data (KBr):  $\tilde{\nu} = 3435$  (br., O–H), 1604 (s, CH=N–N=C), 973 (s, V=O)  $\text{cm}^{-1}$ . UV/Vis ( $\text{CH}_3\text{CN}$  solution):  $\lambda_{\text{max}}$  ( $\epsilon$ ) = 241 (43,900), 273 (21,400), 321 (9500), 540 nm ( $6800 \text{ cm}^{-1} \text{ M}^{-1}$ ).

**[VO(salhyhb)(hq)]:** Yield 0.51 g (1.1 mmol, 55%) in methanol and 0.67 g (1.4 mmol, 70%) in acetonitrile.  $\text{C}_{22}\text{H}_{22}\text{N}_3\text{O}_3\text{V}$  (459.37): calcd. C 57.52, H 4.83, N 9.15; found: C 57.33, H 4.83, N 8.37.  $^1\text{H}$  NMR (400 MHz,  $[\text{D}_6]\text{-DMSO}$ ):  $\delta = 0.80$ – $0.92$  (m, 2 H,  $\text{CH}_2$ ), 1.02–1.10 (m, 4 H,  $\text{CH}_2$ ), 2.15 (t, 2 H,  $^3J = 6.8$  Hz,  $\text{CH}_2\text{C}=\text{O}$ ), 3.10 (t, 2 H,  $\text{CH}_2\text{OH}$ ,  $^3J = 6.6$  Hz), 4.26 (br. s, 1 H, OH), 6.73–6.75 (m, 1 H, arom. CH), 6.97–7.03 (m, 1 H, arom. CH), 7.16–7.21 (m, 1 H, arom. CH), 7.39–7.51 (m, 1 H, arom. CH), 7.56–7.59 (m, 1 H, arom. CH), 7.60–7.69 (m, 2 H, arom. CH), 7.70–7.79 (m, 1 H, arom. CH), 8.09–8.10 (m, 1 H, arom. CH), 8.51–8.53 (m, 1 H, arom. CH), 9.15 (s, 1 H, CH=N) ppm.  $^{13}\text{C}$  NMR (50 MHz,  $[\text{D}_6]\text{-DMSO}$ ):  $\delta = 24.6$ , 25.6 ( $\text{CH}_2$ ), 29.5 ( $\text{CH}_2\text{C}=\text{O}$ ), 31.9 ( $\text{CH}_2\text{CH}_2\text{OH}$ ), 60.3 ( $\text{CH}_2\text{OH}$ ), 110.9, 115.4, 119.5, 120.4, 122.4, 122.9, 128.2, 129.1, 133.2, 135.2, 138.2, 138.6, 146.2 (all arom. CH–C), 154.1 (CH=N), 162.3, 163.3 (both arom. CO–V), 176.0 (CO–V) ppm.  $^{51}\text{V}$  NMR (105 MHz,  $[\text{D}_6]\text{-DMSO}$ ):  $\delta = -472$  ppm ( $\Delta\nu_{1/2} = 358$  Hz).  $^{51}\text{V}$  NMR (105 MHz,  $\text{CDCl}_3$ ):  $\delta = -483$  ppm ( $\Delta\nu_{1/2} = 148$  Hz). Selected IR data (KBr):  $\tilde{\nu} = 3430$  (br., O–H), 1605 (s, CH=N–N=CH), 973 (s, V=O)  $\text{cm}^{-1}$ . UV/Vis ( $\text{CH}_3\text{CN}$  solution):  $\lambda_{\text{max}}$  ( $\epsilon$ ) = 241 (43,200), 273 (20,100), 321 (9100), 540 nm ( $6600 \text{ cm}^{-1} \text{ M}^{-1}$ ).

**Electrochemical Measurements:** Cyclic square-wave voltammetric measurements have been carried out by a three-electrode technique using a home-built computer-controlled instrument based on the PCI 6110-E data acquisition board (National Instruments). The experiments were performed in acetonitrile solutions containing 0.25 M tetra-*n*-butylammonium hexafluorophosphate under a blanket of solvent saturated with argon. The ohmic resistance that had to be compensated for was determined by measuring the impedance of the system at potentials where the faradaic current was negligible. Background corrections were applied only for cyclic voltammograms by subtracting the current curves of the blank electrolyte containing the same concentration of the supporting electrolyte from the experimental cyclic voltammograms. Ag/AgCl was used as the reference electrode in acetonitrile containing 0.25 M tetra-*n*-butylammonium chloride. All potentials reported in this paper refer to the ferrocenium/ferrocene couple, which has been measured at the end of each experiment. The working electrode was a hanging mercury drop ( $m_{\text{Hg-drop}} \approx 4$  mg) generated by a CGME instrument from Bioanalytical Systems Inc., West Lafayette, USA. Theoretical square-wave voltammograms were simulated using the *Digi-Elch* simulation software developed in our group (available via www.DigiElch.de).

**MAS NMR Spectroscopy and Data Evaluation:** Solid-state  $^{51}\text{V}$  MAS NMR experiments were performed at a resonance frequency of 105.19 MHz (9.4 T) with a Bruker AMX 400 spectrometer. The measurements were performed at room temperature, although the

actual sample temperature is a little higher depending on the spinning speed. The magic angle was adjusted using potassium bromide. The spectral width was 1.6 MHz and the pulse width was 1  $\mu\text{s}$ . For each of the compounds, spectra were recorded at two different spinning speeds of 7 and 10 kHz to uniquely determine the isotropic peak and to increase the reliability of the parameters determined from the simulations. The data were processed by Fourier transformation and baseline correction using the MestReC NMR spectroscopic data processing software.<sup>[45]</sup> Isotropic chemical shifts are reported relative to neat  $\text{VOCl}_3$  whose  $^{51}\text{V}$  NMR spectrum was recorded and used as an external referencing standard. The spectral line shape of the  $^{51}\text{V}$  NMR spectra is dominated by the quadrupolar interaction. Compared to this, the influence of the chemical shielding anisotropy (CSA) is relatively small. Therefore, the evaluation of the spectra necessitates numerical simulations, which were performed with the SIMPSON software package.<sup>[46]</sup> The relationship of the quadrupolar and CSA parameters to their principal tensor elements is given by Equation (7).

$$C_Q = \frac{eQV_z}{h} \quad \delta_\sigma = \delta_{\text{iso}} - \delta_{zz}$$

$$\eta_Q = \frac{V_{yy} - V_{xx}}{V_{zz}} \quad \eta_\sigma = \frac{\delta_{xx} - \delta_{yy}}{\delta_s}$$
(7)

where  $\delta_{\text{iso}} = 1/3(\delta_{xx} + \delta_{yy} + \delta_{zz})$  is the isotropic chemical shift and the principal tensor elements of the CSA ( $\delta$ ) and electric field-gradient (V) tensors are defined according to the convention<sup>[47]</sup>  $|\lambda_{zz} - 1/3\text{Tr}(\lambda)| \geq |\lambda_{xx} - 1/3\text{Tr}(\lambda)| \geq |\lambda_{yy} - 1/3\text{Tr}(\lambda)|$  ( $\lambda = \delta, V$ ).  $C_Q$  is the nuclear quadrupolar coupling constant,  $Q$  the nuclear quadrupole moment ( $-4.8 \text{ fm}^2$ ),<sup>[48]</sup>  $e$  the electronic charge, and  $h$  the Planck constant.  $\delta_\sigma$  characterizes the anisotropy of the CSA tensor, whereas  $\eta_Q$  and  $\eta_\sigma$  are the asymmetry parameters of the EFG and CSA tensors, respectively. The full parameter set of the EFG and CSA tensors as well as the Euler angles  $\alpha$ ,  $\beta$ , and  $\gamma$  describing the relative orientation of the principle axis systems of the two tensors at the vanadium center are obtained by least-squares fittings of the simulated and experimental spectra (for details see ref.<sup>[44]</sup>).

Table 3. Crystallographic data and structure refinement parameters for [VO(salhyhb)(hq)].

Empirical formula	$\text{C}_{20}\text{H}_{18}\text{N}_3\text{O}_3\text{V}$
Formula mass [g/mol]	431.31
Crystal size [mm]	$0.3 \times 0.3 \times 0.2$
Crystal system	triclinic
Space group	$P\bar{1}$
$a$ [pm]	1010.08(2)
$b$ [pm]	1042.23(3)
$c$ [pm]	1779.17(6)
$\alpha$ [°]	88.9150(10)
$\beta$ [°]	89.170(2)
$\gamma$ [°]	88.790(2)
$V$ [nm <sup>3</sup> ]	1.87206(9)
$T$ [K]	183(2)
$Z$	4
$\rho_{\text{calcd.}}$ [g/cm <sup>3</sup> ]	1.530
$\mu$ [mm <sup>-1</sup> ]	0.569
$\theta$ range [°]	2.78–27.49
Unique data	8519
Observed data [ $I > 2\sigma(I)$ ]	6635
Parameters	531
Goodness-of-fit on $F^2$	1.029
$R_1$ for observed data	0.0401
$wR_2$ for all data	0.0996

**Crystallographic Study:** Crystallization of [VO(salhyhb)(hq)] from a mixture of methanol and acetonitrile (1:1) afforded violet needle-like crystals suitable for X-ray measurements. The crystallographic data were collected with a Nonius KappaCCD diffractometer using graphite-monochromated Mo- $K_{\alpha}$  radiation (71.073 pm). A summary of the crystallographic and structure refinement data is given in Table 3. The structure was solved by direct methods with SHELXS-97 and was full-matrix least-squares refined against  $F^2$  using the program SHELXL-97.<sup>[49]</sup> Anisotropic thermal parameters were used for all non-hydrogen atoms. The hydrogen atoms of the side-chain hydroxyl groups have been located and isotropically refined, whereas all other hydrogen atoms were calculated and treated as riding atoms with fixed thermal parameters.

CCDC-670707 contains the supplementary crystallographic data for [VO(salhyhb)(hq)]. These data can be obtained free of charge from The Cambridge Crystallographic Centre via <http://www.ccdc.cam.ac.uk/products/csd/request>.

## Acknowledgments

We are grateful to the Deutsche Forschungsgemeinschaft (DFG) for financial support.

- [1] D. C. Crans, J. J. Smee, E. Gaidamauskas, L. Yang, X. Zhang, *Chem. Rev.* **2004**, *104*, 849–902.
- [2] K. H. Thompson, J. H. McNeill, C. Orvig, *Chem. Rev.* **1999**, *99*, 2561–2571.
- [3] H. Sakurai, Y. Kojima, Y. Yoshikawa, K. Kawabe, H. Yasui, *Coord. Chem. Rev.* **2002**, *226*, 187–198.
- [4] R. Wever, W. Hemrika, *Vanadium haloperoxidases in Handbook of Metalloproteins 2* (Eds.: A. Messerschmidt, R. Huber, T. Poulos, K. Wieghardt), p. 1417–1428, John Wiley & Sons, Chichester, **2001**.
- [5] W. Plass, *Angew. Chem.* **1999**, *111*, 960–962; *Angew. Chem. Int. Ed.* **1999**, *38*, 909–912.
- [6] A. Butler, *Curr. Opin. Chem. Biol.* **1998**, *2*, 279–285.
- [7] M. J. Clague, N. L. Keder, A. Butler, *Inorg. Chem.* **1993**, *32*, 4754–4761.
- [8] C. J. Carrano, C. M. Nunn, R. Quan, J. A. Bonadies, V. L. Pecoraro, *Inorg. Chem.* **1990**, *29*, 944–951.
- [9] W. Plass, *Z. Anorg. Allg. Chem.* **1994**, *620*, 1635–1644.
- [10] W. Plass, *Inorg. Chim. Acta* **1996**, *244*, 221–229.
- [11] W. Plass, *Z. Anorg. Allg. Chem.* **1997**, *623*, 461–477.
- [12] W. Plass, *Eur. J. Inorg. Chem.* **1998**, 799–805.
- [13] G. J. Colpas, B. J. Hamstra, J. W. Kampf, V. L. Pecoraro, *Inorg. Chem.* **1994**, *33*, 4669–4675.
- [14] B. J. Hamstra, G. J. Colpas, V. L. Pecoraro, *Inorg. Chem.* **1998**, *37*, 949–955.
- [15] W. Plass, *Coord. Chem. Rev.* **2003**, *237*, 205–212.
- [16] M. R. Maurya, S. Agarwal, C. Bader, D. Rehder, *Eur. J. Inorg. Chem.* **2005**, 147–157.
- [17] H. Michibata, N. Yamaguchi, T. Uyama, T. Ueki, *Coord. Chem. Rev.* **2003**, *237*, 41–51.
- [18] M. J. Manos, A. J. Tasiopoulos, C. Raptopoulou, A. Terzis, J. D. Woollins, A. M. Z. Slawin, A. D. Keramidis, T. A. Kabanos, *J. Chem. Soc., Dalton Trans.* **2001**, 1556–1558.
- [19] L. W. Amos, D. T. Sawyer, *Inorg. Chem.* **1974**, *13*, 78–83.
- [20] T. L. Riechel, D. T. Sawyer, *Inorg. Chem.* **1975**, *14*, 1869–1875.
- [21] A. Giacomelli, C. Floriani, A. O. de Souza Duarte, A. Chiesi-Villa, C. Guastini, *Inorg. Chem.* **1982**, *21*, 3310–3316.
- [22] W. Plass, A. Pohlmann, H.-P. Yozgatli, *J. Inorg. Biochem.* **2000**, *80*, 181–183.
- [23] W. Plass, H.-P. Yozgatli, *Z. Anorg. Allg. Chem.* **2003**, *629*, 65–70.
- [24] A. Roth, A. Buchholz, W. Plass, *Z. Anorg. Allg. Chem.* **2007**, *633*, 383–392.
- [25] J. Becher, I. Seidel, W. Plass, D. Klemm, *Tetrahedron* **2006**, *62*, 5675–5681.
- [26] M. Mancka, W. Plass, *Inorg. Chem. Commun.* **2007**, *10*, 677–680.
- [27] I. Lippold, H. Görls, W. Plass, *Eur. J. Inorg. Chem.* **2007**, 1487–1491.
- [28] A. Pohlmann, S. Nica, T. K. K. Luong, W. Plass, *Inorg. Chem. Commun.* **2005**, *8*, 289–292.
- [29] S. Nica, A. Pohlmann, W. Plass, *Eur. J. Inorg. Chem.* **2005**, 2032–2036.
- [30] U. G. Nielsen, H. J. Jacobsen, J. Skibsted, *J. Phys. Chem. B* **2001**, *105*, 420–429.
- [31] J. M. Miller, L. J. Lakshmi, *J. Mol. Catal. A: Chem.* **1999**, *144*, 451–459.
- [32] D. C. Crans, R. A. Felty, H. Chen, H. Eckert, N. Das, *Inorg. Chem.* **1994**, *33*, 2427–2438.
- [33] D. H. Park, C.-F. Cheng, J. Klinowski, *Bull. Korean Chem. Soc.* **1997**, *18*, 70–75.
- [34] P. D. Hampton, C. E. Daitch, T. M. Alam, E. A. Pruss, *Inorg. Chem.* **1997**, *36*, 2879–2883.
- [35] S. Nica, M. Rudolph, H. Görls, W. Plass, *Inorg. Chim. Acta* **2007**, *360*, 1743–1752.
- [36] S.-X. Liu, S. Gao, *Polyhedron* **1998**, *17*, 81–84.
- [37] S. P. Rath, K. K. Rajak, A. Chakravorty, *Inorg. Chem.* **1999**, *38*, 4376–4377.
- [38] S. Gao, Z.-Q. Weng, S.-X. Liu, *Polyhedron* **1998**, *17*, 3595–3606.
- [39] W. Chen, S. Gao, S.-X. Liu, *Acta Crystallogr., Sect. C: Cryst. Struct. Commun.* **1999**, *55*, 531–533.
- [40] S. P. Rath, K. K. Rajak, S. Mondal, A. Chakravorty, *J. Chem. Soc., Dalton Trans.* **1998**, 2097–2101.
- [41] D. L. Bryce, G. D. Sward, *Magn. Reson. Chem.* **2006**, *44*, 409–450.
- [42] N. Pooransingh, E. Pomerantseva, M. Ebel, S. Jantzen, D. Rehder, T. Polenova, *Inorg. Chem.* **2003**, *42*, 1256–1266.
- [43] K. J. Ooms, S. E. Bolte, J. J. Smee, B. Baruah, D. C. Crans, T. Polenova, *Inorg. Chem.* **2007**, *46*, 9285–9293.
- [44] A. Schweitzer, T. Gutmann, M. Wächter, H. Breitzke, A. Buchholz, W. Plass, G. Buntkowsky, *Solid State Nucl. Magn. Reson.*, DOI: 10.1016/j.ssnmr.2008.02.003.
- [45] J. C. Cobas, F. J. Sardina, *Concepts Magn. Reson.* **2003**, *19A*, 80–96.
- [46] M. Bak, J. T. Rasmussen, N. C. Nielsen, *J. Magn. Reson.* **2000**, *147*, 296–330.
- [47] M. H. Cohen, F. Reif, *Solid State Phys.* **1957**, *5*, 321–438.
- [48] M. R. Hansen, G. K. H. Madsen, H. J. Jakobsen, J. Skibsted, *J. Phys. Chem. B* **2006**, *110*, 5975–5983.
- [49] G. Sheldrick, *SHELXS* and *SHELXL*, University of Göttingen, **1997**.

Received: January 20, 2008  
 Published Online: April 11, 2008